A MIXED LAYER PYROLYSIS MODEL FOR POLYPROPYLENE

by

Kathryn M. Butler
Building and Fire Research Laboratory
National Institute of Standards and Technology
Gaithersburg, MD 20899 USA

Reprinted from the Fire Safety Science. Proceedings. Sixth (6th) International Symposium. International Association for Fire Safety Science (IAFSS). July 5-9, 1999, Poitiers, France, Intl. Assoc. for Fire Safety Science, Boston, MA, Curtat, M., Editor, 313-324 pp, 2000.

A MIXED LAYER PYROLYSIS MODEL FOR POLYPROPYLENE

Kathryn M. Butler
National Institute of Standards and Technology
Gaithersburg, Maryland 20899

ABSTRACT

A one-dimensional model describing the melting, degradation, and bubbling behavior of polypropylene exposed to a high heat flux is presented. The region of vigorous bubbling observed in experiment is represented as a mixed layer of uniform temperature. Temperature profiles and thicknesses of solid, melt, and mixed layers are determined by solving conservation equations supplemented by simple models of turbulent mixing. The results of the model with and without a mixed layer are compared with experiment.

KEY WORDS: Pyrolysis models, gasification, polypropylene

INTRODUCTION

The strength, low cost, and easy processability of polyolefins has led to their widespread use as commodity polymers, with applications ranging from packaging to injection molded parts to structural components. Their behavior in fire is therefore of considerable interest. During thermal degradation, these polymers release volatile gases that add to the available fuel in a fire. A solid understanding of the degradation processes and resulting mass loss rate, critical in the prediction of fire development, is complicated by melting and bubbling phenomena. Polypropylene is studied here as a representative of this important class of materials.

Upon exposure to a high heat flux from above, polypropylene (PP) first melts from a crystalline to an amorphous structure then degrades into volatile gaseous products. These gases are observed to form a surface layer of vigorously growing, moving and bursting bubbles. Although bubbles appear to have a significant effect on the macroscopic thermal and mechanical properties during gasification of a thermoplastic material [1], the mechanisms by which

a bubbling layer affects heat and mass transfer are not well understood. Several possibilities exist. If the bubbling is sufficiently vigorous, the upper layer of melted thermoplastic material could be mixed, such that the temperature throughout the bubbling layer is nearly uniform. Alternatively, the low thermal conductivity of gas compared to that of a liquid could cause an appreciable decrease in heat transport through the bubble layer, denoted by a large temperature gradient. The presence of bubbles may also change the radiative properties of the sample, affecting surface reflectivity and internal radiative processes. An exploration of effects from each of these potential mechanisms accompanied by comparison with experiment will benefit our understanding of the behavior of thermally degrading thermoplastic materials.

Several models have considered the effects of in-depth gasification on the temperature profiles and mass loss rate of pyrolyzing materials [2], [3]. These models neglect the physical effects of bubbles by assuming that gases escape on a timescale short compared to the phenomena of interest. One-dimensional models that incorporate a turbulent layer to study the time evolution of temperature profiles have been developed in oceanography to understand diurnal and seasonal variations in the temperature profile of the upper ocean [4],[5]. In these mixed layer models, the upper layer is assumed to be fully mixed due to turbulent motions driven by solar radiation and wind. Heat and mechanical energy inputs from the surface and mass entrained at the base of the mixed layer are instantaneously redistributed uniformly throughout the layer. The bottom of the layer is marked by a temperature discontinuity, below which the fluid is quiescent.

The model presented in this paper considers the limiting case in which the bubble layer is assumed to be perfectly mixed so that the temperature throughout this layer is uniform. The turbulent motion is generated by the incident heat flux and by the growth, movement, and bursting of bubbles within the mixed layer. The production of bubbles is related to the rate of gasification within the mixed layer, which depends on the temperature through an Arrhenius function. In-depth gasification throughout the entire sample, the phase change from crystalline PP to an amorphous melt, and the thermal properties of the substrate are included.

Finally, the results of the mixed layer model are compared both to an in-depth gasification model that neglects bubble effects and to a recent set of pyrolysis experiments on PP, which is observed to exhibit particularly vigorous bubbling behavior.

MODELS

The geometries of the in-depth gasification model and the mixed layer model are illustrated in Figures (1) and (2) respectively. The mixed layer model consists of five separate regions: the substrate, solid layer, melt layer, entrainment zone, and mixed layer. The thicknesses of these layers are l_b, $l_s(t)$, $l_m(t)$, $\triangle h$, and $h(t)$ respectively. Solid, melt, and mixed layer thicknesses are variables to be solved. The lower surface of the substrate, fixed at $z = -l_b$, is assumed to be adiabatic, and the upper surface of the sample is located at $z = S(t) = l_s + l_m + h$, with the entrainment zone thickness taken in the limit $\triangle h \rightarrow 0$. For the in-depth model, the mixed layer and entrainment zone are eliminated.

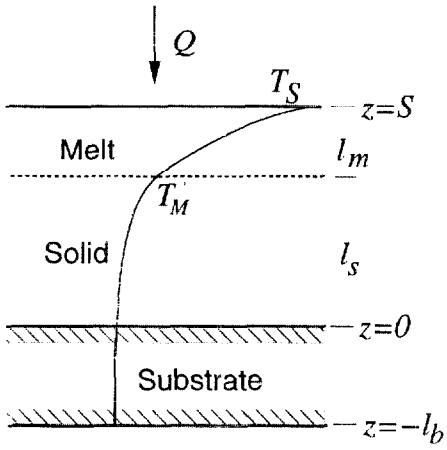

FIGURE 1: In-depth pyrolysis model

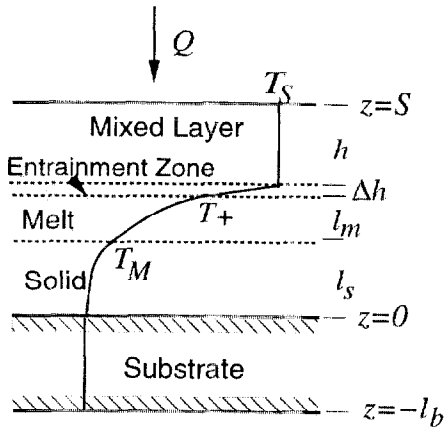

FIGURE 2: Mixed layer model

Although turbulent motion occurs only in the mixed (bubbly) layer, degradation of the polymer is assumed to take place throughout the sample according to an Arrhenius function,

$$\dot{m}(T) = \rho B \exp(-E/RT) \quad , \tag{1}$$

where $\dot{m}$ is the mass loss rate. Transport of gases in this model is of interest only in that it results in thorough mixing of the uppermost layer of liquid. Gases generated below the mixed layer do not disturb the surrounding material, and the escape of all gases to the surroundings is assumed to occur rapidly compared to the timescales of interest.

The evolution of this model in time is depicted in Figure (3).

In-depth Gasification Model

Initially, the sample is a solid slab of material of thickness $S = L$ lying on a substrate of fixed thickness l_b. Using subscripts b and s to indicate substrate and solid quantities respectively, the energy equations to be solved are:

$$\frac{\partial T_b}{\partial t} = \alpha_b \frac{\partial^2 T_b}{\partial z^2} \tag{2}$$

$$\frac{\partial T_s}{\partial t} + W_s \frac{\partial T_s}{\partial z} + \frac{H_v \dot{m}}{\rho_s c_{ps}} = \alpha_s \frac{\partial^2 T_s}{\partial z^2} \tag{3}$$

with initial and lower boundary conditions

$$T_b(z,0) = T_s(z,0) = T_0 \qquad \frac{\partial T_b}{\partial z}\Big|_{z=-l_b} = 0 \text{ (adiabatic)} \tag{4}$$

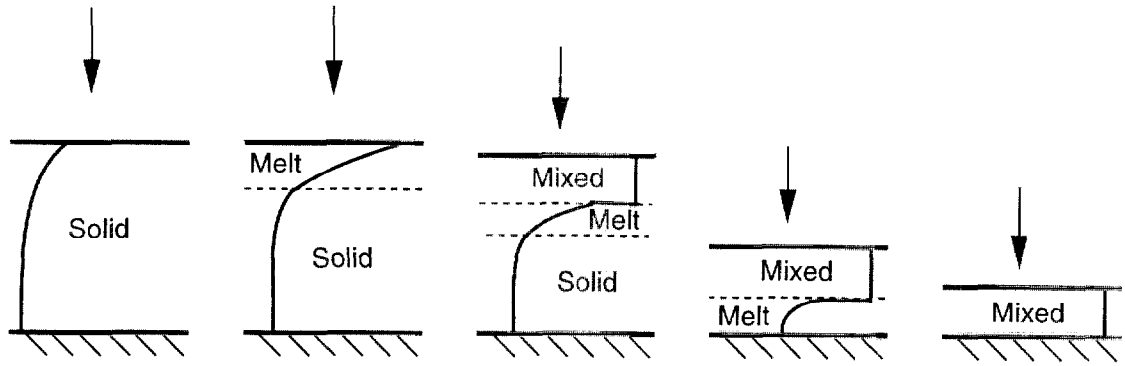

FIGURE 3: Evolution of mixed layer model

$$T_b(0,t) = T_s(0,t) \qquad k_b \frac{\partial T_b}{\partial z}\Big|_{z=0} = k_s \frac{\partial T_s}{\partial z}\Big|_{z=0} \tag{5}$$

where $\alpha = k/\rho c_p$ is the thermal diffusivity, ρ the density, c_p heat capacity, k thermal conductivity, H_v the (positive) heat of vaporization, and T_0 the ambient temperature. Because of in-depth degradation, the velocity of a material element at location z within the solid layer is given by [3]

$$W_s(z,t) = -\int_0^z \frac{\dot{m}(T_s(z,t))}{\rho_s}\, dz \quad . \tag{6}$$

The loss of material results in decrease of the sample thickness at the rate

$$\frac{dS}{dt} = W_s(S,t) = -\int_0^S \frac{\dot{m}(T_s)}{\rho_s}\, dz \quad . \tag{7}$$

before melting begins.

The upper boundary condition for the solid sample is an energy balance with the net incident heat flux until the surface reaches the melting temperature T_M at time t_f^I, at which time the temperature at the top of the solid layer becomes fixed:

$$-k_s \frac{\partial T_s}{\partial z}\Big|_{z=l_s=S} = Q(t) \qquad 0 \leq t < t_f^I \tag{8}$$

$$T_s(l_s,t) = T_M \qquad t_f^I \leq t \tag{9}$$

The net incident heat flux $Q(t)$ includes radiative and convective losses:

$$Q = \epsilon q_0 + \epsilon\sigma\left(T_S{}^4 - T_0^4\right) + h_c\left(T_S - T_0\right) \quad , \tag{10}$$

where ϵ is the emissivity, q_0 the incident heat flux (positive out of the surface), σ the Stefan-Boltzmann constant, h_c the heat transfer coefficient, and T_S the surface temperature.

When the upper surface of the solid reaches the melt temperature T_M, the thermoplastic material begins to undergo a phase change from solid to liquid. The consumption of heat by this phase change must be reflected in the heat flux balance across the interface. Denoting melt variables with the subscript m and introducing the (positive) latent heat of melting by $\triangle i_{sl}$, the melt-solid interface equation can be written as: [6]

$$-k_s \frac{\partial T_s}{\partial z}\bigg|_{l_s} + \rho_s \triangle i_{sl} \frac{dl_s}{dt} = -k_m \frac{\partial T_m}{\partial z}\bigg|_{l_s} \quad , \tag{11}$$

This provides an equation for the interface location l_s, with the initial condition $l_s(t_f^I) = S(t_f^I)$.

In the melt layer, the temperature obeys the heat equation

$$\frac{\partial T_m}{\partial t} + W_m \frac{\partial T_m}{\partial z} + \frac{H_v \dot{m}}{\rho_m c_{pm}} = \alpha_m \frac{\partial^2 T_m}{\partial z^2} \tag{12}$$

subject to the initial and lower boundary conditions:

$$T_m\left(z, t_f^I\right) = T_M \qquad T_m\left(l_s, t\right) = T_M \quad . \tag{13}$$

In addition to the vertical motion caused by the loss of underlying material due to in-depth gasification, the velocity in the melt must also account for any change in density between the solid and liquid states. The velocity at location z in the melt is therefore given by

$$W_m(z,t) = -\int_0^{l_s} \frac{\dot{m}(T_s)}{\rho_s}\, dz - \int_{l_s}^{z} \frac{\dot{m}(T_m}{\rho_m}\, dz + \left(1 - \frac{\rho_s}{\rho_m}\right) \frac{dl_s}{dt} \quad . \tag{14}$$

In the absence of a mixed layer, the upper boundary condition for the melt is given by:

$$-k_m \frac{\partial T_m}{\partial z}\Big|_{z=S} = Q(t) \qquad \text{where } S = l_s + l_m \quad . \tag{15}$$

At this point, the model accounts for in-depth gasification, a phase change from solid to melt, and the internal vertical velocities caused by these two phenomena. The results from this in-depth gasification model will be compared later in this paper with the results of the mixed layer model to investigate the effects of a turbulent bubble layer on the behavior of a pyrolyzing thermoplastic material.

Mixed Layer

Once the sample has developed a liquid layer, released gases may begin to form bubbles near the surface. In the mixed layer model, this region is treated as a fluid layer of uniform temperature with density equal to that of the melt. Swelling due to internal bubbles is not included.

In addition to the temperature profiles in solid and melt layers and the location of the phase interface, the model must determine the melt and mixed layer thicknesses and the mixed layer temperature. The upper boundary condition for the melt temperature must reflect the interface with the entrainment layer. The necessary equations are derived from consideration of the mixed and entrainment layers.

The development of this mixed layer model parallels the modeling of the oceanic mixed layer [4], and begins with the conservation equations for the three-dimensional motion within the mixed and entrainment layers. Assuming an incompressible Newtonian fluid, the equations of mass, momentum, and energy are

$$\frac{\partial U_i}{\partial x_i} = -\frac{\dot{m}}{\rho_m} \quad , \tag{16}$$

$$\rho_m \left(\frac{\partial U_i}{\partial t} + U_j \frac{\partial U_i}{\partial x_j} \right) = -\frac{\partial P}{\partial x_i} + g\rho_m \hat{\beta}(T - \widehat{T_S})\delta_{i3} + \rho_m \nu \nabla^2 U_i \quad , \tag{17}$$

$$\rho_m c_{pm} \left(\frac{\partial T}{\partial t} + U_j \frac{\partial T}{\partial x_j} \right) + H_v \dot{m} = \frac{\partial}{\partial x_j} k_m \frac{\partial T}{\partial x_j} \quad . \tag{18}$$

where P is the gage pressure, g is acceleration due to gravity, ν is kinematic viscosity, and $\dot{m} = \dot{m}(T) = \rho_m B \exp(-E/RT)$. Subscripts i and j indicate the three coordinate directions $x_1, x_2, x_3 = x, y, z$ respectively, with velocities $U_1, U_2, U_3 = U, V, W$. Coordinate z is in the vertical direction. The momentum equation includes the standard Boussinesq approximation, in which density variations are neglected except in the buoyancy term. There, density is given by

$$\rho = \rho_m \left[1 - \hat{\beta}(T - \widehat{T_S}) \right] \quad , \tag{19}$$

where ρ_m is the melt density at the quasi-steady state temperature $\widehat{T_S}$ of the mixed layer during pyrolysis and $\hat{\beta}$ is the coefficient of thermal expansion.

The mixed layer turbulence is converted to mean quantities through Reynolds averaging. Assume that there is an timescale τ long enough to adequately average horizontal and vertical disturbances in the mixed and entrainment layers but short enough to follow the evolution of the averaged quantities of interest. A field quantity such as $T(x, y, z, t)$ can be written as the sum of mean and fluctuating components,

$$T(x, y, z, t) = \overline{T}(z, t) + \theta'(x, y, z, t) \quad , \tag{20}$$

where the mean, or Reynolds average, has been defined as

$$\overline{T} = \frac{1}{\tau} \int_0^\tau T \, dt \tag{21}$$

and the deviation from the mean is denoted by a prime. Averaged quantities depend only on z and t since homogeneity is assumed in the horizontal directions x and y. Since fluctuations are both positive and negative, $\overline{\theta'} = 0$.

Similarly, velocity components U_i and pressure P are written in terms of mean and fluctuating components as $U_i(x,y,z,t) = \overline{U}_i(z,t) + u'_i(x,y,z,t)$ and $P(x,y,z,t) = \overline{P}(z,t) + p'(x,y,z,t)$. Due to horizontal homogeneity, only the z component of mean velocity is nonzero:

$$\overline{W}(z,t) = -\int_0^{l_s} \frac{\dot{m}(T_s)}{\rho_s}\,dz - \int_{l_s}^{l_s+l_m} \frac{\dot{m}(T_m)}{\rho_m}\,dz + \left(1 - \frac{\rho_s}{\rho_m}\right)\frac{dl_s}{dt} - \frac{[z-(S-h)]\,\dot{m}(T_S)}{\rho_m} \quad (22)$$

where T_S is the uniform temperature in the mixed layer. The velocity of the upper surface can be obtained from this expression as

$$\begin{aligned} \frac{dS}{dt} &= \frac{dl_s}{dt} + \frac{dl_m}{dt} + \frac{dh}{dt} = \overline{W}(S,t) \\ &= -\int_0^{l_s} \frac{\dot{m}(T_s)}{\rho_s}\,dz - \int_{l_s}^{l_s+l_m} \frac{\dot{m}(T_m)}{\rho_m}\,dz + \left(1 - \frac{\rho_s}{\rho_m}\right)\frac{dl_s}{dt} - \frac{h\dot{m}(T_S)}{\rho_m} \quad . \end{aligned} \quad (23)$$

Conservation equations for the mean quantities are derived by substituting the sum of mean and fluctuating components for U_i, T, and P into the conservation equations and Reynolds-averaging the result. Equations for the turbulent quantities are then obtained by subtracting these averaged equations from the original equations.

Of particular interest to the transport of heat is the mean energy equation,

$$\frac{\partial \overline{T}}{\partial t} + \frac{\partial \overline{W}\,\overline{T}}{\partial z} + \frac{\dot{m}}{\rho_m}\overline{T} + \frac{\partial}{\partial z}\overline{w'\theta'} + \frac{H_v \dot{m}(\overline{T})}{\rho_m c_{pm}} = \alpha_m \frac{\partial^2 \overline{T}}{\partial z^2} \quad . \quad (24)$$

This equation enables heat to be transported from the surface of the sample through the turbulent mixed and entrainment layers and into the quiescent melt and solid layers. The key to this process is the term $\partial\overline{w'\theta'}/\partial z$, which represents the local divergence of the turbulent heat flux in the vertical direction. Through this term the net heat flux incident to the sample surface is converted into the turbulence of the mixed layer, then converted back into a mean heat flux at the base of the entrainment layer.

At the upper surface of the mixed layer, the incident heat flux is considered to be redistributed instantaneously into uniform turbulent motion throughout the mixed layer. The turbulent heat flux at $z = S$ is therefore equal to the heat flux imposed on the surface,

$$\overline{w'\theta'}\,\Big|_S = \frac{Q}{\rho_m c_{pm}} \quad . \quad (25)$$

Below the entrainment layer, the turbulent heat flux is equal to zero. The transport of heat through the mixed and entrainment layers may be followed by integrating the mean energy

equation (24) over various regions to determine the value of $\overline{w'\theta'}$ at intermediate locations. In summary, heat energy transported through the mixed layer is lost to gasification reactions and to increase the uniform mixed layer temperature. Between the mixed layer and the quiescent melt, heat goes into entraining the melt and thus deepening the mixed layer. The heat energy remaining after these expenditures heats the melt and solid layers and fuels the phase change from solid to liquid.

The upper boundary condition for melt temperature is determined by integration of the mean energy equation from just below the entrainment zone to the top of the mixed layer:

$$\alpha_m \frac{\partial T_m}{\partial z}\bigg|_{l_s+l_m} = -\frac{Q}{\rho_m c_{pm}} - h\left(\frac{dT_S}{dt} + \frac{H_v \dot{m}(T_S)}{\rho_m c_{pm}}\right) - (T_S - T_+)\left(\frac{dh}{dt} + \frac{h\dot{m}(T_S)}{\rho_m}\right) \quad . \quad (26)$$

Note that under the conditions $h = 0$ and $T_S = T_+$, which would be expected to hold in the absence of the mixed layer, boundary condition (15) is recovered.

To complete the mathematical description of this problem, two additional equations are required. These equations are obtained by considering the kinetic and heat energy required to maintain a turbulent state in the mixed layer. An equation for turbulent energy is derived by multiplying the turbulent momentum equation (the mean momentum equation subtracted from the full equation (17)) by the fluctuating velocity u'_i:

$$u'_i\left\{\frac{\partial u'_i}{\partial t} + w'\frac{\partial \overline{W}}{\partial z}\delta_{i3} + \overline{W}\frac{\partial u'_i}{\partial z} + u'_j\frac{\partial u'_i}{\partial x_j} - \overline{u'_j\frac{\partial w'}{\partial x_j}}\delta_{i3} = -\frac{1}{\rho_m}\frac{\partial p'}{\partial x_i} + g\hat{\beta}\theta'\delta_{i3} + \nu\nabla_2 u'\right\} \quad (27)$$

Taking a Reynolds average of this equation produces a balance equation for turbulent kinetic energy, which is then integrated over mixed and entrainment layers from $z_0 = S - h - \triangle h$ to S to provide the equation

$$g\hat{\beta}\int_{z_0}^{S}\overline{w'\theta'}dz = G + D - \nu\frac{Q}{\rho_m c_{pm}}\frac{\dot{m}(T_S)E}{\rho_m R{T_S}^2} \quad . \quad (28)$$

Since the value of the turbulent heat flux $\overline{w'\theta'}$ as a function of position is known, this equation can be written in terms of the problem variables as

$$g\hat{\beta}\left[\frac{Qh}{\rho_m c_{pm}} + \frac{h^2}{2}\left(\frac{dT_S}{dt} + \frac{H_v\dot{m}(T_S)}{\rho_m c_{pm}}\right) + \alpha_m(T_S - T_+)\right] = G + D - \nu\frac{Q}{\rho_m c_{pm}}\frac{\dot{m}(T_S)E}{\rho_m R{T_S}^2} \quad (29)$$

In these equations, integrated products of turbulent quantities are collected into G, the net production of turbulent kinetic energy, and D, the turbulent energy dissipation. Terms included in G represent the production of turbulence due to Reynolds stresses acting on the mean shear, the production or loss of turbulence due to the interaction of the mass lost during gasification with Reynolds stresses and turbulent pressure, and energy transport by turbulent diffusion and viscous stresses. The connection between turbulent kinetic energy and turbulent heat flux is due to buoyancy.

In order to satisfy closure for this equation, terms G and D must be written as functions of the mean quantities. In upper ocean models, measurements have provided a basis for the representation of these terms. In the absence of similar data for bubbling, the turbulent energy production and dissipation are assumed to be proportional to the rate of loss of material due to gasification in the mixed layer:

$$G + D = A_{KE}\, h\, \dot{m}(T_S) \quad . \tag{30}$$

The final equation needed to solve this problem is derived by summing the turbulent energy equation multiplied by the perturbed vertical velocity $w'\delta_{i3}$ with the z-component of the turbulent momentum equation (equation (27) divided by u'_i) multiplied by the perturbed temperature θ'. The Reynolds average of the resulting equation is a balance equation for turbulent heat flux. Integrating over mixed and entrainment layers from $z0 = S - h - \Delta h$ to S provides the equation

$$\int_{z_0}^{S} \frac{\partial \overline{w'\theta'}}{\partial t} dz + \overline{W w'\theta'}\,\Big|_{z_0}^{S} + \int_{z_0}^{S} \frac{\overline{w'\theta'}}{\overline{T}} \frac{H_v \dot{m}(\overline{T})}{\rho_m c_{pm}} \frac{E}{R\overline{T}} = B \quad , \tag{31}$$

where the production of turbulent heat flux is represented by B, whose terms include vertical transport due to turbulent diffusion, viscous stresses and thermal diffusivity and production of turbulent heat flux due to turbulent motions interacting with the mean shear, mean temperature gradient, gasification, turbulent pressure, and buoyancy. Replacing $\overline{w'\theta'}$ with known expressions, equation (31) can be written as

$$\begin{aligned} &\alpha_m \left(\frac{dT_S}{dt} - \frac{dT_+}{dt} \right) + \left(\frac{dS}{dt} - \frac{dh}{dt} \right) (T_S - T_+) \left(\frac{\dot{m}(T_S) h}{\rho_m} + \frac{dh}{dt} \right) \\ &\quad + \frac{h^2}{2} \frac{d}{dt} \left(\frac{dT_S}{dt} + \frac{H_v \dot{m}(T_S)}{\rho_m c_{pm}} \right) + h \frac{dS}{dt} \left(\frac{dT_S}{dt} + \frac{H_v \dot{m}(T_S)}{\rho_m c_{pm}} \right) + \frac{dS}{dt} \frac{Q}{\rho_m c_{pm}} \\ &\quad + \frac{H_v}{\rho_m c_{pm}} \alpha_m \left(\dot{m}(T_S) - \dot{m}(T_+) \right) = B \end{aligned} \tag{32}$$

The turbulent heat flux production is assumed to depend linearly on the rate of gasification and mixed layer temperature:

$$B = A_{HF}\, T_S\, \dot{m}(T_S) \quad . \tag{33}$$

The mixed layer model has been implemented by means of an iterative solution procedure using Mathematica.[1] At each time step the energy equations for substrate, solid, and melt regions are solved using Crank-Nicolson and the most recent set of layer thicknesses. The resulting temperature gradients are then inserted into a set of ODE's that calculates thicknesses and mixed layer temperature. The procedure is repeated until convergence is achieved.

[1] Certain trade names and company products are mentioned in the text in order to specify adequately the procedure used. In no case does such identification imply recommendation or endorsement by the National Institute of Standards and Technology, nor does it imply that the products are necessarily the best available for the purpose.

RESULTS

Calculations for polypropylene were carried out using both the in-depth gasification model with no bubble effects and the mixed layer model. Parameter values used for PP were: $\rho_s = 0.90$ g/cm^3, $k_s = 0.00117$ J/cm-K, $c_{ps} = 2.5$ J/g-K, $B = 2.4 \times 10^{14}$ s^{-1}, $E/R = 26207$ K, $T_M = 444$ K, $\Delta i_{sl} = 207$ J/g, $H_v = 800$ J/g, $\epsilon = 0.92$, $r = 0.08$, and $h_c = 0.001$ W/cm^2-K. Since results were to be compared with experiments performed in the NIST gasification chamber [8], other input values having to do with the substrate and physical setup were as follows: $\rho_b = 0.2$ g/cm^3, $k_b = 7.69 \times 10^{-4} + 1.51 \times 10^{-6}T - 1.63 \times 10^{-9}T^2 + 8.64 \times 10^{-12}T^3$ J/cm-K, $c_{pb} = 0.76$ J/g-K, $l_b = 5.1$ cm, $L = 2.54$ cm, $q_0 = -4$ W/cm^2, and $T_0 = 298$ K. The turbulence coefficients A_{HF} and A_{KE} were chosen to provide a mixed layer of significant thickness relative to the melt layer (roughly one-sixth the melt thickness). Given the uncertainties in the turbulent model formulation and values, the interest here is in understanding the trends introduced by this approach to bubble modeling.

The plots in Figures (4) and (5) show the thicknesses of the total PP sample and each layer within the sample as functions of time for both the in-depth gasification model and the mixed layer model. In both cases, a quasi-steady state situation is reached after roughly two minutes. From this time until the solid has melted completely, the melt and mixed layer thicknesses are nearly constant as pyrolysis takes place.

In Figure (6), the upper surface temperature for the in-depth model is plotted as a function of time along with the temperatures of the mixed layer and at the top of the melt layer, just below the discontinuity in the mixed layer model. It is interesting that the temperature T_+ at the top of the melt layer reaches a maximum before decreasing to its quasi-steady state value. If the timing is compared with that of the layer thicknesses in Figure (5), the decrease in T_+ is seen to coincide with the initial development of the mixed layer. During entrainment, heat energy goes into deepening the mixed layer, therefore the heat flux entering the melt layer is reduced. Once the mixed layer thickness becomes steady, the temperature T_+ also levels off.

The presence of the turbulent bubble layer decreases the surface temperature as well as the temperatures within the melt and solid layers. However, the temperature decrease is not sufficient to counter the fact that the entire mixed layer, though thin, is gasifying at a high rate, and the mass loss rate is actually increased by the mixed layer. This is shown in Figure (7). Once the solid layer has melted, the mass loss rate increases significantly due to the rapidly thinning sample. The effect of the melt-solid phase change is to limit the temperature at the bottom of the sample to the melt temperature, resulting in a flattening of the mass loss rate plot until the solid has disappeared, at which time the slope becomes nearly discontinuous. This effect is not reflected in the experimental data, which shows a steadily increasing mass loss rate with time. This discrepancy may be due at least in part to the assumption that the incident heat flux is absorbed at the surface. The addition of in-depth absorption to the model would be expected to slow the initial temperature increases and therefore reduce the mass loss rate at early times. Including changes of physical properties of solid and melt with temperature will also modify the mass loss rate curves.

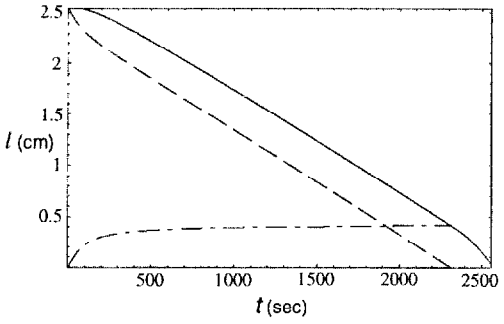

FIGURE 4: Thicknesses of total sample S (solid line), solid layer l_s (dashed line), and melt layer l_m (dot-dash) vs. time for in-depth gasification model.

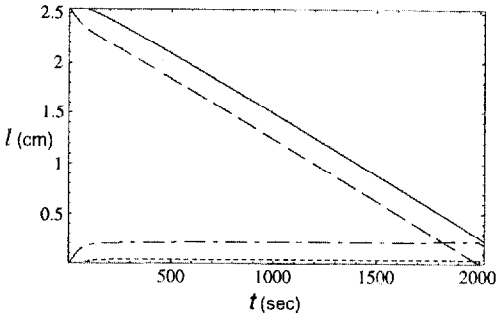

FIGURE 5: Thicknesses of total sample S (solid line), solid layer l_s (dashed line), melt layer l_m (dot-dash), and mixed layer h (dotted line) vs. time for mixed layer model.

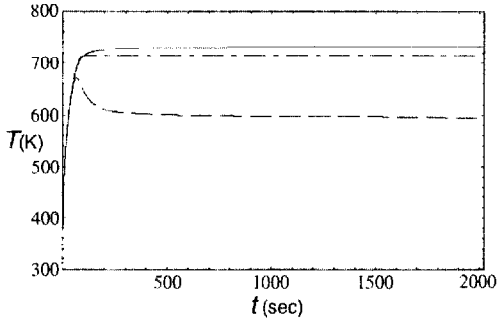

FIGURE 6: Temperature as a function of time for the upper surface of the in-depth gasification model (solid line), mixed layer T_S (dot-dash), and top of the melt layer T_+ (dashed line).

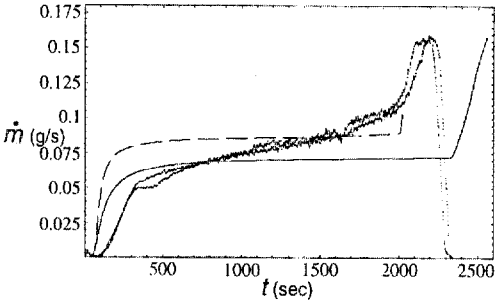

FIGURE 7: Mass loss rate as a function of time for the in-depth gasification model (solid line), mixed layer model (dashed line), and two sets of experimental results (points).

CONCLUSIONS

A mixed layer model to describe the possible effects of bubbling on heat transport through thermoplastic materials subjected to a steady heat flux has been developed. Thorough mixing of the fluid near the surface is assumed to result from the rapid growth, motion, and bursting of bubbles. The model includes thermal effects of the substrate, radiative and convective heat losses from the surface, and a solid-melt phase change. The phase change results in a nearly constant mass loss rate with time instead of the steady increase in time displayed by experiment, suggesting that indepth absorption of incident heat flux and perhaps a more detailed description of polymer softening and melting chemistry are worth investigating. The presence of a turbulent bubble layer is found to decrease the surface and interior temperatures but increase the total mass loss rate. However, a significant improvement in prediction of mass loss rate with time has not been demonstrated by this application of a mixed layer bubble model.

Further exploration of how the presence of a bubble layer affects thermal conductivity, radiation, and mass transport will improve our understanding of the impact of bubbles on pyrolysis and burning of thermoplastic materials.

ACKNOWLEDGMENTS

The author would like to thank Kenneth Steckler, Takashi Kashiwagi, Thomas Ohlemiller, Howard Baum, and William Mell of NIST for helpful discussions on this project.

REFERENCES

[1] Kashiwagi, T. and Ohlemiller, T.J., "A Study of Oxygen Effects on Non-flaming Transient Gasification of PMMA and PE During Thermal Irradiation," Nineteenth Symposium (International) on Combustion, The Combustion Institute, 815–823, 1982.

[2] Vovelle, C., Delfau, J.-L., Reuillon, M., Bransier, J., and Laraqui, N., "Experimental and Numerical Study of the Thermal Degradation of PMMA," Comb. Sci. & Tech. 53:187–201, 1987.

[3] Staggs, J.E.J., "A Theoretical Investigation into Modelling Thermal Degradation of Solids Incorporating Finite-Rate Kinetics," Comb. Sci. & Tech. 123:261–285, 1997.

[4] Denman, K.L., "A Time-Dependent Model of the Upper Ocean," J. Phys. Ocean. 3:173–183, 1973.

[5] Niiler, P.P., "Deepening of the Wind-Mixed Layer," J. Marine Res. 33:405–422, 1975.

[6] Kaviany, M., Principles of Convective Heat Transfer, Springer-Verlag, New York, 1994, p. 559.

[7] Steckler, K.D., private communications.

[8] Ritchie, S.J., Steckler, K.D., Hamins, A., Cleary, T.G., Yang, J.C., and Kashiwagi, T., "The Effect of Sample Size on the Heat Release Rate of Charring Materials," Proceedings of the 5th Int. Symp. on Fire Safety Science, 177–188, 1997.